Published in final edited form as:

Eur J Cancer. 2016 May ; 59: 57–64. doi:10.1016/j.ejca.2016.02.012.

Renal Cell Carcinoma: A nomogram for the CT imaging-inclusive prediction of indolent, non-clear cell renal cortical tumors

Christoph A. Karlo, MD[1], **Lei Kou, MA**[2], **Pier Luigi Di Paolo, MD**[1], **Michael W. Kattan, PhD**[2], **Robert J. Motzer, MD**[3], **Paul Russo, MD**[4], **Satish K. Tickoo, MD**[5], **Oguz Akin, MD**[1], and **Hedvig Hricak, PhD**[1]

[1] Genitourinary Imaging Group, Department of Radiology, MSKCC*, New York, USA

[2] Department of Quantitative Health Sciences, Cleveland Clinic, Cleveland, USA

[3] Genitourinary Oncology Service, Department of Medicine, MSKCC, New York, USA

[4] Urology Service, Department of Surgery, MSKCC, New York, USA

[5] Genitourinary Pathology, Department of Pathology, MSKCC, New York, USA

Abstract

Aim—To develop a nomogram from clinical and computed tomography (CT) data for pre-treatment identification of indolent renal cortical tumors.

Patients and Methods—1,201 consecutive patients underwent dedicated contrast-enhanced CT prior to nephrectomy for a renal cortical tumor between January 2000 and July 2011. Two radiologists evaluated all tumors on CT for size, necrosis, calcification, contour, renal vein invasion, collecting system invasion, contact with renal sinus fat, multicystic tumor architecture, nodular enhancement, and the degree of nephrographic phase enhancement. CT and clinical predictors (gender, BMI, age) were incorporated into the nomogram. We employed multivariable logistic regression analysis to predict tumor type and internally validated the final model using the data from reader 1. External validation was performed by using all data from reader 2. We applied Wilcoxon rank sum test and Fisher's exact test to investigate for differences in tumor size, BMI, age, and differences in CT imaging features between patients with aggressive and those with indolent tumors.

Results—63.6% (764/1’201) of patients had clear-cell or other aggressive non-clear-cell RCC (i.e. papillary RCC type 2, unclassified RCC) and 36.4% (437/1’201) had indolent renal cortical tumors (i.e. papillary RCC type 1, chromophobe RCC, angiomyolipoma, or oncocytoma). On CT, indolent tumors were significantly smaller ($p<0.001$) than aggressive tumors and significantly associated with well-defined tumor contours ($p<0.001$). Aggressive RCC were significantly

Corresponding author: Christoph A. Karlo, MD, Department of Radiology, University Hospital Zurich, Ramistrasse 100, 8091 Zurich, Switzerland, Christoph.Karlo@usz.ch, Tel: +41 44 255 1723, Fax: +41 44 255 1725.

* MSKCC = Memorial Sloan Kettering Cancer Center

associated with necrosis, calcification, renal vein invasion, collecting system invasion, contact with renal sinus fat, multicystic tumor architecture, and nodular enhancement (all, $p<0.001$). The nomogram's C-index was 0.823 after internal and 0.829 after external validation.

Concluding Statement—We present a nomogram based on 1,201 patients combining CT features with clinical data for the prediction of indolent renal cortical tumors. When externally validated, this nomogram resulted in a concordance index of 0.829.

Keywords

CT; Computed Tomography; Renal Cell Carcinoma; RCC; Clear Cell; Chromophobe; Papillary; Oncocytoma; Angiomyolipoma; Nomogram

Introduction

Renal cell carcinoma (RCC) comprises a heterogeneous group of renal epithelial cancers, which may be classified into clear cell, papillary, chromophobe and other, either unclassified or less common subtypes.[1, 2] Among the more common subtypes, clear cell RCC has the worst prognosis, while papillary and chromophobe RCC may be considered indolent tumors, because they remain localized and are therefore often curable.[3] Aside from malignant renal cortical tumors, the benign oncocytoma and lipid-poor angiomyolipoma frequently mimic clear cell RCC on medical imaging and thus substantially contribute to the fact that about 10%-20% of renal cortical tumors resected because RCC is initially suspected prove to be benign.[4]

Given these differences in aggressiveness of histological subtypes of RCC and the tendency of oncocytomas and lipid-poor angiomyolipomas to mimic clear cell RCC, improved medical imaging strategies are needed for identifying indolent renal cortical tumors preoperatively, so that unnecessary invasive biopsy and/or treatment can be avoided in the future. A number of recent studies investigated the ability of computed tomography (CT), the most commonly used imaging modality for patients with renal cortical tumors, to differentiate not only between subtypes of RCC, but also between RCC and oncocytoma or the more prevalent angiomyolipoma.[5-9] A common finding of most of the studies was that the degree of early enhancement during the corticomedullary phase was largest for clear cell RCC followed by oncocytoma, chromophobe RCC, and papillary RCC [10]. However, since both clear cell RCC and oncocytoma demonstrate peak enhancement during the corticomedullary phase, these two entities may not be reliably differentiated by the exclusive use of contrast enhancement analyses.

Today, nomograms are often used to assess the level of risk posed by a patient's cancer. Yet to date, no nomograms that incorporate morphologic imaging features (other than tumor size) have been developed for distinguishing clear-cell or unclassified RCC from more indolent or benign types of renal cortical tumors.

Therefore, the purpose of this study was to develop a nomogram that combines clinical data with CT features for the non-invasive, pretreatment identification of indolent, non-clear-cell renal cortical tumors.

Material (Patients) and Methods

Patients

Our institutional review board approved this retrospective HIPAA-compliant study, and waived the requirement for informed consent. Patients were included in the study upon fulfilment of all of the following criteria:

(a) Nephrectomy performed at our institution (a tertiary care cancer center) between January 2000 and July 2011 for localized clear cell RCC, localized chromophobe RCC, localized papillary RCC types 1 and 2, localized unclassified RCC, oncocytoma, or angiomyolipoma.

(b) Pre-operative contrast-enhanced CT of the abdomen and pelvis performed at our institution using a dedicated kidney CT protocol and available in DICOM format through our institution's PACS.

(c) Availability of clinical information (i.e., gender, age, body mass index [BMI], clinical presentation [i.e. symptomatic or asymptomatic]) as well as histopathology reports indicating the histopathological tumor type through our institution's electronic medical records system.

As shown in the patient selection flowchart (**Figure 1**), a total of 1,201 patients were eligible for inclusion in this study.

CT Image Acquisition & Analysis

All patients underwent multiphasic contrast-enhanced CT imaging prior to nephrectomy using either 16- or 64- detector row CT scanners (General Electric Medical Systems, Milwaukee, USA) at a constant tube voltage setting of 120 kV. All CT studies consisted of non-enhanced imaging of the abdomen as well as contrast-enhanced imaging during the nephrographic (delay, 90 sec) and urographic (delay, 3 min) phases after the application of 150 mL of iodinated contrast agent (Omnipaque 300, GE Healthcare) at a constant flow rate of 3.5 mL/sec. In patients with creatinine levels above 1.3, the amount of contrast agent was reduced to 100 mL. Reconstruction slice thickness was 2.5 mm for all CT studies. In patients who had more than one tumor (8.2% [99/1’201]), the largest lesion was chosen for analysis.

Without knowledge of neither histopathological nor clinical information, two board-certified radiologists performed all image analyses using commercially available PACS software (Centricity, General Electric Medical Systems; Milwaukee, USA). Both radiologists independently assessed all images for the following features:

(a) The largest tumor diameter on the transverse CT image during the nephrographic phase;

(b) The presence of necrosis (a tumor was deemed necrotic if ill-defined, hypodense areas of the tumor did not enhance at all during the nephrographic and urographic phases);

(c) The presence of calcifications within the tumor.

(d) The nature of the tumor's contour, recorded as either ill-defined or well-defined (a tumor contour was deemed ill-defined if the tumor was not clearly delineated from all adjacent anatomical structures on all transverse imaging planes during the nephrographic phase);

(e) Evidence of venous invasion, defined as a filling defect caused by tumor extension into the branches of the renal vein on nephrographic phase images;

(f) Evidence of collecting system invasion, defined as a filling defect within the collecting system on urographic phase images;

(g) Evidence of tumor contact with renal sinus fat, defined as direct contact between the tumor and the adipose tissue of the renal sinus;

(h) Evidence of multicystic tumor architecture;

(i) Evidence of heterogeneous (i.e. peripheral-nodular) enhancement during the nephrographic phase.

Figure 2 illustrates examples of all features.

In addition, one reader measured the Hounsfield Unit density of each tumor's most solid component on unenhanced and nephrographic-phase, contrast-enhanced CT images as baseline parameters to calculate the degree of nephrographic phase enhancement.

Statistical Analysis

The objective of this project was to develop a pre-operative model for the prediction of the following indolent renal cortical tumor types: papillary RCC type 1, chromophobe RCC, oncocytoma, and angiomyolipoma. On the contrary, we classified these tumor types as aggressive: clear cell RCC, unclassified RCC, and papillary RCC type 2. From here on we refer to the above mentioned groups as “indolent tumors” and “aggressive tumors”. For the calculation of the predictive model, we combined clinical predictors (i.e. gender, age, and BMI), and predictors derived from CT imaging (i.e., tumor size, necrosis, calcification, tumor contour, renal vein invasion, collecting system invasion, tumor contact with renal sinus fat, multicystic tumor architecture, nodular enhancement pattern, and the degree of nephrographic phase enhancement).

Multivariable logistic regression analysis was employed to predict tumor type. All clinical and CT variables, as assessed by reader 1, were included in an initial model. A step-down method based on the concordance index (C-index) was used to select a subset of the predictors to achieve a relatively parsimonious model with the maximum C-index, for the final model. The final model was internally validated using data from reader 1. External validation was performed by using all data from reader 2. The C-index was used as an indicator to present predictive accuracy, which is identical to the area under the receiver operating characteristic (ROC) curve. The C-index ranges from 0.5 (no predictive power) to 1 (perfect prediction). Calibration of the nomogram was assessed graphically by smoothing a scatter plot of the predicted probabilities and the observed outcomes. The plot illustrates how far the prediction is from the actual tumor type (the closer the line is to the 45-degree line, the better the nomogram predicts).

Wilcoxon rank sum test was applied to investigate for differences in tumor size, body mass index, age and the degree of nephrographic phase enhancement between patients with aggressive and those with indolent tumors. Fisher's exact test was applied to investigate for differences between aggressive and indolent tumors with respect to the distribution of necrosis, calcifications, tumor contour, renal vein invasion, collecting system invasion, tumor contact with renal sinus fat, presence of multicystic tumor architecture, and nodular enhancement.

Results

The patients' clinical and CT Imaging characteristics are summarized in **Table 1**. A multivariable logistic regression model was developed to predict binary outcome of tumor type (aggressive versus indolent tumors). Ten out of fifteen predictors were included in the final model. Clinical presentation was dropped, because it reduced the concordance index. The predictors included in the final model were: age, gender, BMI, CT necrosis, CT calcifications, CT tumor contour, CT renal vein invasion, CT collecting system invasion, CT presence of multicystic tumor architecture, CT tumor contact with renal sinus fat, CT nodular enhancement, CT tumor size, and CT nephrographic enhancement. Interreader agreement for all features was excellent (Table 2). While the results of reader 1 were used to construct the nomogram, the results of reader 2 served to validate the nomogram.

Patients with indolent tumors, when compared to those with aggressive tumors, had a significantly lower BMI (28.7±5.5 vs. 30.2±6.2; p=0.0001). No significant differences were found for age (p=0.1311) and gender (p=0.0545) between patients with indolent and aggressive tumors. Indolent tumors were significantly smaller (4.0±2.5 cm vs. 4.4±2.6 cm; p=0.0001) than aggressive tumors. Regarding the predictors derived from CT imaging, ill-defined tumor contour, presence of necrosis and calcifications, evidence of renal vein invasion, evidence of collecting system invasion, contact with renal sinus fat, presence of multicystic tumor architecture, nodular enhancement were significantly associated with aggressive tumors (all, p<0.001; **Table 3**). Nephrographic phase enhancement was significantly higher in aggressive tumors when compared to indolent tumors (289.8% ±169.8% vs. 202.5±154.6%; p<0.0001).

The graphic nomogram derived from the final regression model is presented in **Figure 3**. The C-index based on internal validation of the nomogram was 0.823, and 0.829 for external validation. The calibration plot is presented in **Figure 4**, odds ratios in **Table 4**.

Discussion

We developed a nomogram for the pre-treatment identification of indolent, non-clear cell renal cortical tumors based on clinical and CT imaging data derived from 1,201 patients. When externally validated, the nomogram led to a concordance index of 0.829.

Nomograms have previously been designed to predict patient survival based on data acquired before or after treatment of renal tumors. Lane et al. developed a pre-treatment nomogram that incorporated clinical data with tumor size on CT to predict the presence of malignant tumors in patients with small renal masses. This nomogram was designed using

data from 862 patients with solid renal lesions 7 cm or less in size. When internally validated, the nomogram had a bootstrap-corrected C-index of 0.644. The nomogram resulted in an even lower C-index of 0.557 for the prediction of potentially aggressive histology.[11] Our nomogram, which incorporated fewer clinical variables but a larger number of CT imaging features and focused specifically on the identification of indolent tumors, resulted in a higher C-index of 0.829.

Raj et al. developed a pre-operative nomogram for the prediction of metastatic recurrence at 12 years based on data from 2517 patients [12]. This nomogram, which resulted in a C-index of 0.8, included gender, clinical presentation (i.e. incidental, localized, systemic), as well as tumor size, lymphadenopathy and evidence of necrosis on imaging. Our nomogram (which aimed to predict tumor histology rather than recurrence) included a larger number of predictors from CT, namely, tumor size, tumor contour (either ill- or well-defined), evidence of renal vein invasion, evidence of tumor contact with renal sinus fat, presence multicystic tumor architecture, and evidence of heterogeneous enhancement during the nephrographic phase – a feature that may be understood to imply the presence of necrosis within a tumor.

We included the definition of a tumor's contour because we hypothesized that indolent tumors would display clearer delineation towards the normal kidney parenchyma than would aggressive tumors; in keeping with this expectation, we discovered that aggressive tumors displayed ill-defined contours significantly more often than did indolent tumors (**Table 3**). We also found, as we had expected, that renal vein invasion was significantly more common among aggressive tumors than among indolent tumors (**Table 3**). Therefore, the presence of renal vein invasion on CT imaging may be considered a strong predictor for aggressive tumor. In addition, we included direct contact between the renal cortical tumor and the renal sinus fat because this feature is known as a surrogate marker for invasion of muscular venous branches of the renal vein, and therefore stage T3a.[13, 14] Interestingly, we found that contact between renal cortical tumors and renal sinus fat was significantly more common among aggressive tumors than among indolent tumors. However, size may have been a confounding factor influencing this finding, given that, if a renal cortical tumor grows large, it will eventually establish contact with the renal sinus fat, and in our study, aggressive tumors were significantly larger than indolent tumors (4.4±2.6 cm vs. 4.0±2.5 cm; p=0.0001). However, it has previously been shown that small renal cortical tumors clearly separated from the renal sinus fat were significantly less likely to present as stage T3a during histopathological analysis.[13, 14]

In our study, aggressive tumors demonstrated a peripheral nodular enhancement pattern during the nephrographic phase significantly more often than did indolent tumors. This finding may be explained by an observation from a prior study, which indicated that nodular enhancement patterns were related to mutations of the Von Hippel Lindau (VHL) gene. The VHL gene is a trigger mutation in clear cell RCC and leads to an up-regulation of hypoxia-inducing factors, thereby resulting in increased angiogenesis, which can be identified on contrast-enhanced CT imaging.[15]

We also found that patients with aggressive tumors had a significantly higher body mass index. This rather interesting finding was in line with the results of a prior study by

Lowrance et al., who demonstrated that among patients with renal cortical tumors, obesity was associated with an elevated risk of clear cell RCC [16].

Our study had the following limitations: First, we included CT exams acquired on different CT scanners. However, our analysis was retrospective, and we aimed to keep the sample size as large as possible for the construction of the nomogram. Moreover, we exclusively included CT exams that had been performed at our institution using a dedicated renal mass protocol. Second, histopathology specimens were not re-analysed by a pathologist for this study, although all our nephrectomies, as a routine, are signed out by a dedicated genitourinary pathologist only. Third, the amount of contrast material applied in each patient was not weight corrected; therefore, CT features associated with enhancement could have been affected by the different, non-weight-adapted doses of contrast material. Fourth, as long as they remain small, most angiomyolipomas that can be identified as such clearly on imaging are followed with imaging rather than surgically resected. Therefore, angiomyolipomas in this study were either large or highly atypical, meaning that they did not demonstrate macroscopic fat on CT imaging.

In conclusion, we designed an easy-to-use nomogram that appears to be reasonably accurate for the pre-treatment prediction of indolent, non-clear cell renal cortical tumors. This nomogram in its current form does not have the power to replace biopsy but may contribute to decision making processes in the management of patients with renal cortical tumors.

Acknowledgements

The authors acknowledge the help of Ada Muellner in editing the manuscript. Ada Muellner is the editor at the Department of Radiology, Memorial Sloan Kettering Cancer Center.

Role of the Funding Sources

The founding sources did not have any roles in the project.

Funding: RSNA R&E Foundation Grant RF1304, Swiss National Science Foundation Ambizione Grant PZ00P3_147988, and NIH/NCI Cancer Center Support Grant P30 CA008748. None of the funding sources were actively involved in this project.

References

1. Truong LD, Shen SS. Immunohistochemical diagnosis of renal neoplasms. Archives of pathology & laboratory medicine. 2011; 135:92–109. [PubMed: 21204715]
2. Kovacs G, Akhtar M, Beckwith BJ, Bugert P, Cooper CS, Delahunt B, et al. The Heidelberg classification of renal cell tumours. The Journal of pathology. 1997; 183:131–3. [PubMed: 9390023]
3. Moch H, Gasser T, Amin MB, Torhorst J, Sauter G, Mihatsch MJ. Prognostic utility of the recently recommended histologic classification and revised TNM staging system of renal cell carcinoma: a Swiss experience with 588 tumors. Cancer. 2000; 89:604–14. [PubMed: 10931460]
4. Asnis-Alibozek AG, Fine MJ, Russo P, McLaughlin T, Farrelly EM, LaFrance N, et al. Cost of care for malignant and benign renal masses. The American journal of managed care. 2013; 19:617–24. [PubMed: 24304211]
5. Sasiwimonphan K, Takahashi N, Leibovich BC, Carter RE, Atwell TD, Kawashima A. Small (<4 cm) renal mass: differentiation of angiomyolipoma without visible fat from renal cell carcinoma utilizing MR imaging. Radiology. 2012; 263:160–8. [PubMed: 22344404]

6. Hindman N, Ngo L, Genega EM, Melamed J, Wei J, Braza JM, et al. Angiomyolipoma with minimal fat: can it be differentiated from clear cell renal cell carcinoma by using standard MR techniques? Radiology. 2012; 265:468–77. [PubMed: 23012463]

7. Cardone G, D'Andrea A, Piscioli I, Scialpi M. Fat-poor angiomyolipoma and renal cell carcinoma: differentiation with MR imaging and accuracy of histopathologic evaluation. Radiology. 2012; 265:979–80. author reply 80-1. [PubMed: 23175553]

8. Kim JY, Kim JK, Kim N, Cho KS. CT histogram analysis: differentiation of angiomyolipoma without visible fat from renal cell carcinoma at CT imaging. Radiology. 2008; 246:472–9. [PubMed: 18094264]

9. Vargas HA, Chaim J, Lefkowitz RA, Lakhman Y, Zheng J, Moskowitz CS, et al. Renal cortical tumors: use of multiphasic contrast-enhanced MR imaging to differentiate benign and malignant histologic subtypes. Radiology. 2012; 264:779–88. [PubMed: 22829683]

10. Young JR, Margolis D, Sauk S, Pantuck AJ, Sayre J, Raman SS. Clear cell renal cell carcinoma: discrimination from other renal cell carcinoma subtypes and oncocytoma at multiphasic multidetector CT. Radiology. 2013; 267:444–53. [PubMed: 23382290]

11. Lane BR, Babineau D, Kattan MW, Novick AC, Gill IS, Zhou M, et al. A preoperative prognostic nomogram for solid enhancing renal tumors 7 cm or less amenable to partial nephrectomy. The Journal of urology. 2007; 178:429–34. [PubMed: 17561141]

12. Raj GV, Thompson RH, Leibovich BC, Blute ML, Russo P, Kattan MW. Preoperative nomogram predicting 12-year probability of metastatic renal cancer. The Journal of urology. 2008; 179:2146–51. discussion 51. [PubMed: 18423735]

13. Karlo CA, Donati OF, Marigliano C, Tickoo SK, Hricak H, Russo P, et al. Role of CT in the assessment of muscular venous branch invasion in patients with renal cell carcinoma. AJR American journal of roentgenology. 2013; 201:847–52. [PubMed: 24059374]

14. Karlo CA, Di Paolo PL, Donati OF, Russo P, Tickoo S, Hricak H, et al. Renal cell carcinoma: role of MR imaging in the assessment of muscular venous branch invasion. Radiology. 2013; 267:454–9. [PubMed: 23418001]

15. Karlo CA, Di Paolo PL, Chaim J, Hakimi AA, Ostrovnaya I, Russo P, et al. Radiogenomics of clear cell renal cell carcinoma: associations between CT imaging features and mutations. Radiology. 2014; 270:464–71. [PubMed: 24029645]

16. Lowrance WT, Thompson RH, Yee DS, Kaag M, Donat SM, Russo P. Obesity is associated with a higher risk of clear-cell renal cell carcinoma than with other histologies. BJU international. 2010; 105:16–20. [PubMed: 19583732]

Highlights

- Our nomogram contains clinical and imaging derived data.
- We aimed to differentiate aggressive from indolent types of renal cortical tumors.
- The nomogram resulted in an externally validated C-index of 0.829.
- Aggressive renal cancer was more likely to be in contact with renal sinus fat.
- Indolent renal tumors were more likely homogeneous in enhancement on imaging.

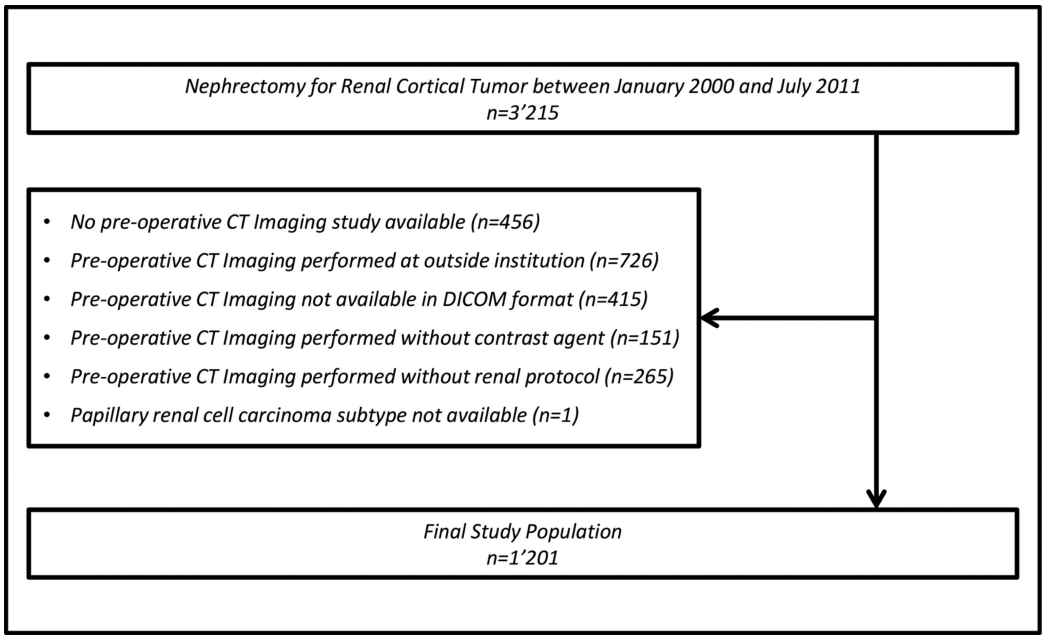

Figure 1.
Patient selection flowchart.

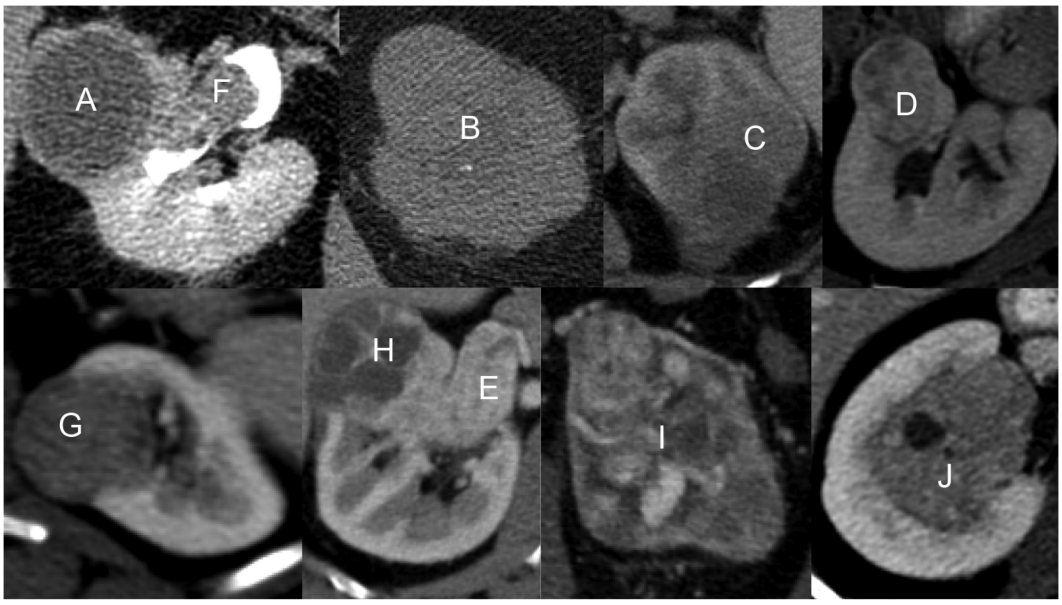

Figure 2.

CT imaging features as assessed by both readers: A, necrosis; B, calcifications; C, Ill-defined tumor margin; D, well-defined tumor margin; E, renal vein invasion; F, collecting system invasion; G, contact with the renal sinus; H, evidence of multicystic tumor architecture; I, nodular enhancement pattern; and J, solid enhancement pattern.

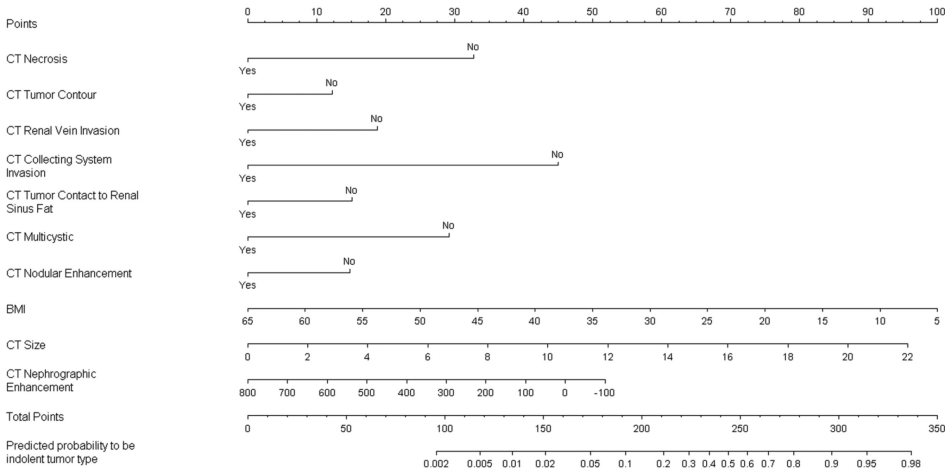

Figure 3.

Nomogram for predicting the probability of indolent renal cortical tumor histology. Points were assigned by drawing a straight line from the appropriate spot on the level of each predictor up to the “Points” level; a line was then drawn straight down from the appropriate spot on the “Total points” level to determine the corresponding predicted probability of indolent tumor histology.

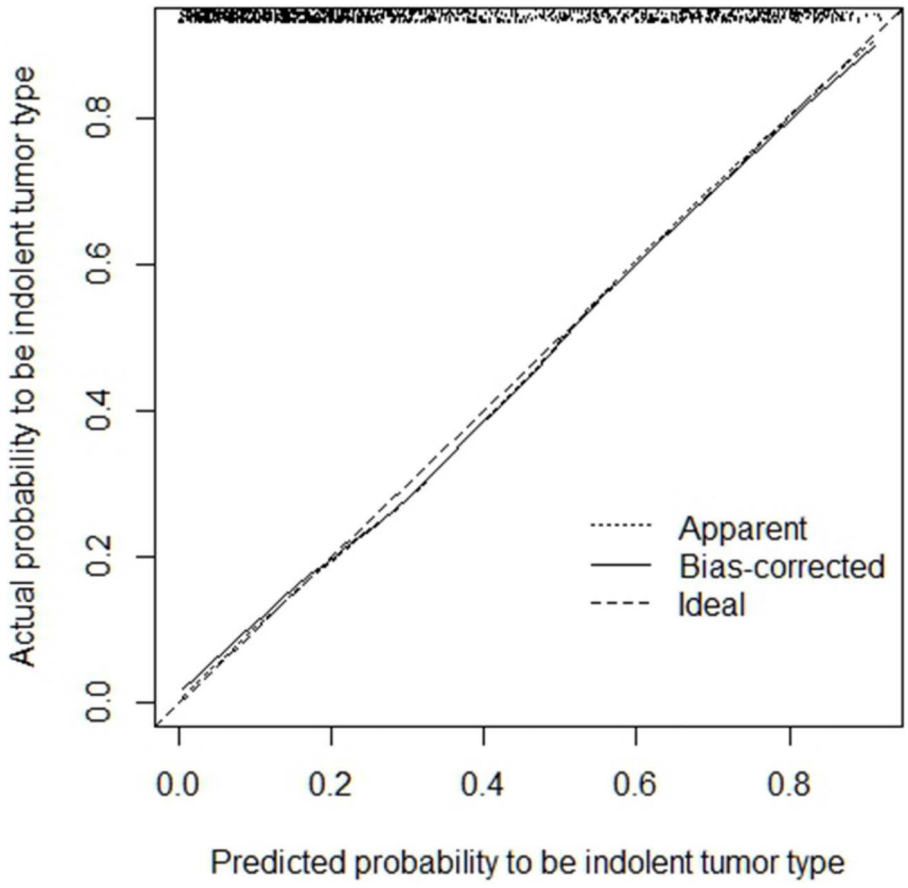

Figure 4.
Nomogram calibration plot. The dots close to the top illustrate the distribution of predicted probabilities for indolent tumors.

Table 1

Clinical data & Parameters derived from CT

Total Number of Patients		**N=1'201**	
Gender	*Male*	62.4% (749/1'201)	
	Female	37.6% (452/1'201)	
BMI *(mean ± SD, range)*		29.7 ± 6 (9.6-61.8)	
Age *(mean ± SD, range; in years)*		60.4 ± 11.9 (22-95)	
Clinical Presentation	*Symptomatic*	17.7% (213/1'201)	
	Asymptomatic	82.3% (988/1'201)	
Histopathological Tumor Type			
Clear cell renal cell carcinoma		56% (673/1'201)	
Papillary renal cell carcinoma	*Type 1*	12.8% (154/1'201)	
	Type 2	2.3% (28/1'201)	
Chromophobe renal cell carcinoma		12.3% (148/1'201)	
Oncocytoma		8.8% (105/1'201)	
Unclassified renal cell carcinomas		5.3% (63/1'201)	
Angiomyolipoma		2.5% (30/1'201)	
Type of Nephrectomy	*Partial*	75.4% (906/1'201)	
	Radical	24.6% (295/1'201)	
CT Predictors		***Reader 1***	***Reader 2***
Tumor Size (mean ± SD, range, in cm)		4.3 ± 2.6 (0.9-21.5)	4.3 ± 2.6 (0.9-21.5)
Necrosis		65% (781/1'201)	64.7% (777/1'201)
Calcification		17.6% (211/1'201)	17.9% (215/1'201)
Tumor Contour	*Ill-defined*	44.5% (535/1'201)	49.4% (593/1'201)
	Well-defined	55.5% (666/1'201)	50.6% (608/1'201)
Renal Vein Invasion		6.7% (80/1'201)	5% (60/1'201)
Collecting System Invasion		9.7% (116/1'201)	6.6% (79/1'201)
Tumor Contact with Renal Sinus Fat		65.8% (790/1'201)	66.7% (801/1'201)
Multicystic Tumor Architecture		13% (156/1'201)	11.5% (138/1'201)
Nodular Enhancement		45.3% (544/1'201)	43.7% (525/1'201)

Table 2

Interreader Agreements

CT Predictor	Kappa Value	Lower 95% CI	Upper 95% CI
Necrosis	0.982	0.97	0.993
Calcifications	0.937	0.911	0.963
Contour	0.900	0.875	0.925
Renal Vein Invasion	0.636	0.536	0.737
Collecting System Invasion	0.794	0.729	0.859
Tumor Contact to Renal Sinus Fat	0.957	0.94	0.975
Multicystic	0.923	0.889	0.956
Nodular Enhancement	0.961	0.946	0.977

CI = Confidence Interval

Table 3

Comparison of clinical and CT imaging predictors in clear cell and non-clear cell tumors

Predictors		Indolent Tumor Type		*p* *
		Yes	No	
Body Mass Index (mean±SD; range)		28.7±5.5 (9.6-51.2)	30.2±6.2 (10-61.8)	0.0001
Age (mean±SD; range)		61±11.9 (22-95)	60±11.9 (32-85)	0.1311
Gender	*Male*	58.8% (257/437)	64.4% (492/764)	0.0545
	Female	41.2% (180/437)	35.6% (272/764)	
CT Tumor Size (mean±SD; range; in cm)		4±2.5 (0.9-16.7)	4.4±2.6 (1-21.5)	0.0001
CT Nephrographic Enhancement (mean±SD; range)		202.5±154.6 (−33.3-706.2)	289.8±169.8 (−43.8-754.5)	<0.0001
Necrosis	no	63.2% (276/437)	81.2% (620/764)	<0.0001
	yes	36.8% (161/437)	18.8% (144/764)	
Calcifications	no	86.7% (379/437)	80% (611/764)	0.0031
	yes	13.3% (58/437)	20% (153/764)	
Tumor Contour	Well-Defined	70.3% (307/437)	47% (359/764)	<0.0001
	Ill-Defined	29.7% (130/437)	53% (405/764)	
Renal Vein Invasion	no	98.2% (429/437)	90.6% (692/764)	<0.0001
	yes	1.8% (8/437)	9.4% (72/764)	
Collecting System Invasion	no	1.6% (7/437)	85.7% (655/764)	<0.0001
	yes	98.4% (430/437)	14.3% (109/764)	
Tumor Contact With Renal Sinus Fat	no	48.5% (212/437)	26% (199/764)	<0.0001
	yes	51.5% (225/437)	74% (565/764)	
Multicystic tumor architecture	no	95.9% (419/437)	81.9% (626/764)	<0.0001
	yes	4.1% (18/437)	18.1% (138/764)	
Nodular Enhancement Pattern	no	75.1% (328/437)	43.1% (329/764)	<0.0001
	yes	24.9% (109/437)	56.9% (435/764)	

* derived from Wilcoxon rank sum test & Fisher's exact test; SD = standard deviation;

Table 4

Odds ratios for the prediction of indolent renal cortical tumors – final selection of predictors.

Predictors	Odds Ratio	Lower 0.95	Upper 0.95
Body Mass Index	0.6174	0.5185	0.7351
CT Tumor Size	1.6071	1.3402	1.927
CT Necrosis	0.253	0.1815	0.3527
CT Contour	0.5986	0.4411	0.8124
CT Renal Vein Invasion	0.4546	0.1833	1.1272
CT Collecting System Invasion	0.1516	0.061	0.3765
CT Tumor Contact to Renal Sinus Fat	0.5297	0.382	0.7344
CT Multicystic Tumor Architecture	0.2942	0.1665	0.5198
CT Nodular Enhancement	0.5384	0.3815	0.7599